



Localised light delivery on melanoma cells using optical microneedles

XIAOBIN WU,^{1,2}  JONGHO PARK,¹ SIU YU A. CHOW,^{1,3} MARIA CARMELITA Z. KASUYA,¹ YOSHIHO IKEUCHI,¹  AND BEOMJOON KIM^{1,*}

¹*Institute of Industrial Science, The University of Tokyo, Tokyo, Japan*

²*Department of Precision Engineering, School of Engineering, The University of Tokyo, Japan*

³*Department of Chemistry and Biotechnology, School of Engineering, The University of Tokyo, Japan*

*bjoonkim@iis.u-tokyo.ac.jp

Abstract: Light-based therapy is an emerging treatment for skin cancer, which has received increased attention due to its drug-free and non-invasive approach. However, the limitation of current light therapy methods is the inability for light to penetrate the skin and reach deep lesions. As such, we have developed a polylactic acid (PLA) microneedles array as a novel light transmission platform to perform *in vitro* evaluation regarding the effect of light therapy on skin cancer. For the first time, we designed and fabricated a microneedle array system with a height fixation device that can be installed in a cell culture dish and an LED array for blue light irradiation. The effect of the blue light combined with the microneedles on cell apoptosis was evaluated using B16F10 melanoma cells and analyzed by Hoechst staining. Our results demonstrate that blue light can be transmitted by microneedles to skin cells and effectively affect cell viability.

© 2022 Optica Publishing Group under the terms of the [Optica Open Access Publishing Agreement](#)

1. Introduction

Skin cancer is one of the most common forms of cancer, and the number of diagnosed patients increases every year. There are two main types of skin cancer: 1) non-melanoma, which includes squamous cell carcinoma (SCC) and basal cell carcinoma (BSS), and 2) melanoma. Other less common cancer types include atypical fibroxanthoma and skin gland cancer [1–4]. Among them, melanoma is recognized as the most aggressive skin cancer because of its fast proliferation rate and high lethality. Melanoma can be classified into five levels based on the depth of invasions of melanoma cells, where melanoma cells were found from the epidermis until dermis. Therefore, various treatment methods have been proposed, including surgical resection, chemotherapy, radiotherapy, photodynamic therapy, immunotherapy, and targeted therapy to treat melanoma in different levels. However, some ineffective results achieved by most of these treatments are attributed to the high resistance by melanomas. Therefore, the combination strategies, such as a combination of light-based therapy with these treatments has been proposed to improve therapeutic effect for melanoma treatment in early stage [5–7].

In the combination therapies, light-based therapy like phototherapy, also known as light therapy based on photobiomodulation, has been used as an anti-tumor treatment method because of its non-invasive and no drug resistance. Photosensitizers or photon receptors in cells such as flavins, porphyrins, and mitochondria can produce reactive oxygen species (ROS) under specific wavelengths, leading to cell death (apoptosis) [8,9]. In addition, light-emitting diode (LED) therapy has gradually become a novel anti-cancer treatment method because of its large-area irradiation, low cost, and high energy features. In particular, in terms of the effects of different wavelengths, various types of LEDs have been used in the treatment of clinical skin diseases, such as acne, inflammation, and psoriasis [10,11]. Although LED light therapy for melanoma has not

been widely used in clinical practice, previous studies have confirmed that blue light irradiation at a certain intensity can significantly inhibit the proliferation of melanoma cells [12,13].

Meanwhile, the skin presents a complex heterogeneous medium having various optical characteristics. When light irradiates the skin surface, it is reflected, absorbed, and scattered by haemoglobin, melanin, filamentous proteins, etc. Hence, light cannot always penetrate the skin to the desired target treatment depth. In particular, blue light with high energy photons can only reach a depth of less than 0.5 mm [14,15]. Red light and near-infrared (NIR) light can penetrate deeper. However, mitochondria do not react to these wavelengths [16]. Moreover, increasing the total energy of the light source to deliver more light into the skin results to epidermal burns [8]. Therefore, by providing a light access directly to the desired skin depth, the effect of LED treatment will be greatly improved, and reduce epidermal burns.

To provide the access to the dermis layer using optical delivery, optical microneedles was first proposed in 2016 [17]. Micron-scale dimension needles used in a patch (a microneedle array) represent a novel biomedical device designed to pierce the stratum corneum (outer skin layer) for viable medical applications involving the epidermis and dermis layers of skin [18,19]. With the development of micron-sized fabrication, microneedle can be fabricated by electro-drawn, micro molding, 3D printing, lithography based on various applications [19,20]. At the same time, the development of various new medical materials has also led to the development of the microneedle industry. In general, dissolving or biodegradable microneedles have been developed and proved able to release drug molecules into the skin after dermal insertion instead of traditional materials like metal, silicon [19–23]. With the refinement of manufacturing technology and materials, applications of microneedle is no longer limited to drug delivery, and optical delivery is gaining attention as a painless and convenient means that facilitates photon transport. Thus, various applications have been investigated, such as single optical microneedle fibers, optical microneedle mounted on surgical forceps, and an optical lens combined with microneedles [17,20,24,25,29]. In 2021, Coppola *et al.* reported that biocompatible and biodegradable drug delivery microneedles fabricated by PLGA are able to focus and transmit light [20]. The ability of several optical microneedles has been proposed using simulation and analysis of light transmission; however, only a few studies were performed *in vivo* and *in vitro*. Previous study proposed the integration of an optical microneedle with surgical forceps to treat pituitary

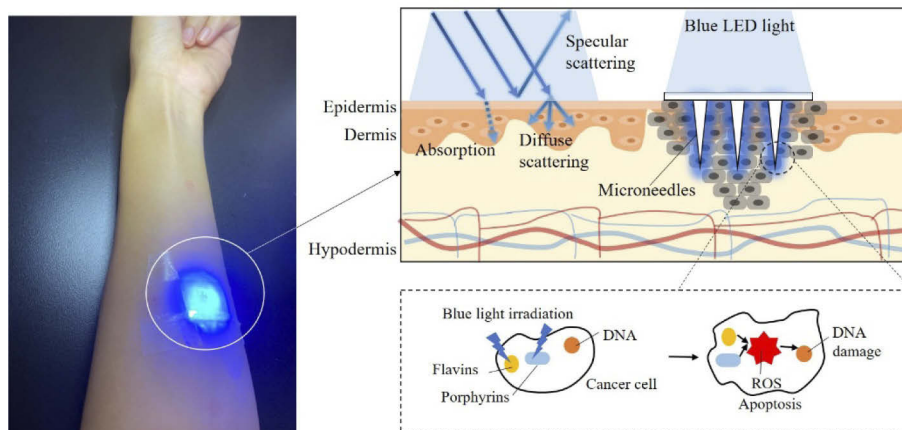


Fig. 1. Schematic of the difficulties associated with light delivery in skin tissue and how directional access provided by the optical microneedle patch overcomes these issues to deliver light through the epidermis and trigger the apoptosis of melanoma cells in the dermis layer.

adenomas by introducing ultraviolet (UV light) [24]. However, treatments of skin disease using optical microneedles *in vitro* has never been investigated before.

In this study, we developed a polylactic acid (PLA) microneedle array with high transparency as a novel light transmission platform for *in vitro* evaluation of the effect of light therapy on skin melanoma. As Fig. 1 shows, an array of transparent microneedles is pierced into the skin to perfect the transmission of light under the skin. When the blue light hits the melanoma cells, the photons are absorbed and the reactive oxygen ions produced promote apoptosis of the cells themselves, thus killing the cancer cells with blue light. Therefore, we designed and fabricated a novel fixed-height microneedle array system that can be installed in a cell culture dish. A commercially available blue LED (wavelength of 467 nm) array for blue light irradiation was integrated in the study. The effect of blue light irradiated through microneedles on cell proliferation was then evaluated using B16F10 murine melanoma cells. This is the first report of the design and fabrication of optical microneedles incorporated with LED array to investigate the effect of light therapy *in vitro*.

2. Materials and methods

2.1. Materials in this study

The cell irradiation system consists of a 12-LED array fitted to a standard 12-well plate (1 LED per well), four 3D-printed support brackets, and a portable power bank supply. The LED array has 12 LEDs (blue light 467 nm, Jiangsu Everstar Electronics Co., Ltd, green light 518 nm, Linkman Co., Ltd., red light 630 nm, ROHM Co., Ltd.), a printed circuit board (PCB) (Sunhayato Corp.), lead-type multilayer ceramic capacitor (Murata Manufacturing Co., Ltd.), voltage regulator (New Japan Radio Co., Ltd.), micro USB DIP connector, and a 5 V output portable power bank. The 3D-printed support bracket was designed using Autodesk Fusion 360 and printed by a LulzBot TAZ printer using transparent PLA (Mutoh Industries, Ltd.).

PLA microneedles were fabricated using a biodegradable and transparent polymer material, polylactic acid (PLA). For this study, PLA (3D850) pellets were purchased from Nature3D (Nature Works LLC, USA) and the polydimethylsiloxane (PDMS) negative mold material, silicone elastomer base solution, and silicone elastomer curing agent SILPOT184 were purchased from Dow Corning Corporation (Dow Inc., USA).

For the porcine skin penetration test, porcine ear skin was purchased from FunaKoshi, Japan (K1270). Staining was churned out using a 10 mg/mL methylene blue (M9140, Sigma-Aldrich, USA) solution. After staining, the porcine skin was wiped with ethanol (24194, Sigma-Aldrich, USA).

B16-F10 melanoma cells were purchased from the Cell Engineering Division CELL BANK (Tokyo, Japan). Dulbecco's Modified Ham's F-12 Eagle Medium (DMEM/F12, without phenol red and without glutamine) was purchased from Thermo Fisher Scientific (USA). Foetal bovine serum (FBS) was purchased from JRH Biosciences, Inc. (USA). The antibiotic-antimycotic (ABAM) solution was purchased from Nacalai Tesque, Inc. (Japan). Trypsin/EDTA (without phenol red) was purchased from Invitrogen (Thermo Fisher Scientific, USA). Trypan blue (0.4% in 0.81% sodium chloride and 0.06% potassium phosphate dibasic solution), cell counting chamber slides, and cell culture treated 12-well plates were purchased from Thermo Fisher Scientific (USA). A 12-well cell culture insert (8.0 μ m PET translucent) was purchased from SABEU GmbH & Co. (Germany). Hoechst 33342 used to stain DNA was purchased from MilliporeSigma (USA), propidium iodide (PI) solution from Dojindo (FUJIFILM Corporation, Japan), and paraformaldehyde (PFA) from Electron Microscopy Sciences (USA).

2.2. Cell culture

B16-F10 melanoma cells were used for *in vitro* experiments. Cells were grown in DMEM/F-12 (Dulbecco's Modified Eagle Medium/Nutrient Mixture F-12) supplemented with 10% FBS (Fetal bovine serum) and 1% ABAM (Antibiotic-Antimycotic). Cells were cultured under standard culture conditions (5% CO₂ in a 37 °C humidified incubator). All cells were detached using 0.25% trypsin/EDTA and passaged twice per week to prevent cells from reaching high confluency. The medium was refreshed every second day.

2.3. LED irradiation

Blue LEDs with a wavelength of 467 nm at a power of 6.5 mW/cm² were used for some *in vitro* experiments. The LED setup was designed to irradiate a 12-well plate. Printed circuit boards (PCBs) for each LED array were patterned into three columns and four rows corresponding to the 12-well plate configuration. Twelve LEDs were connected in parallel. Two capacitors and a low-loss three-terminal regulator ensured that the 5 V mobile power supply met the 3.3 V required by each LED. The average height of each LED was 40 mm above the bottom of each well. The viewing angle of a blue LED was 18°. For dose calculations, the power density measured using an integrating sphere was multiplied by the irradiation time.

Light doses based on irradiation time were calculated from the power densities measured using integrating spheres for the blue, green, and red LED arrays. The irradiation doses are listed in [Supplement 1](#).

A voltage regulator was added to obtain a stable input voltage that met the LED requirements. Each array (467 nm, 518 nm, and 630 nm wavelengths) was fixed on four 3D-printed support brackets. The brackets can support the LED array at a fixed distance from the culture dish, and can ventilate to dissipate heat, which eliminates the influence of heat-induced factors on the experimental results. Through the designed shape of the bracket, the LEDs on the PCB board can correspond to the center of each well 40 mm above each well, ensuring uniformity and covering the entire well with light irradiation. The viewing angles ($2\theta_{1/2}$) for the blue, green, and red LEDs were 18°, 15°, and 12°, respectively. All LED support brackets were manufactured with slits at the ends to allow airflow for heat dissipation purposes. A single LED array was driven using a standard power supply at constant voltage, which, in principle, allows the modulation of the light intensity. Two capacitors and a low-loss three-terminal regulator ensured that the 5 V mobile power supply met the required voltage by each LED. Under these conditions, the light intensity was measured using a physical sensor (an integrating sphere) to crosscheck the observed values. Integrating sphere which is designed to capture all the light that enters is usually used to measure LED because of its divergent property. A Petri dish containing 1 mL of culture fluid was placed at the entrance of the integrating sphere photometer and the LED light source was placed 40 cm away from the Petri dish. This height corresponds to the set-up height of the cell experiment. The light entering the culture medium and refracted into the integrating sphere is captured and used as the light intensity value of the experimental light source [16]. The properties and dose calculations of the arrays are presented in [Supplement 1](#). In all biological experiments, doses were calculated based on the power density measured by the integrating sphere. The power density measured using the integrating sphere (W/cm²) was multiplied by the irradiation time (s) to determine the dose. Several parameters of the cell irradiation system were evaluated and are reported in [Supplement 1](#), including the actual wavelength and half-bandwidth of the LEDs used and the average light power density obtained at the bottom of each well of the 12-well plate. Light values were measured based on power density.

2.4. Cell viability

B16F10 melanoma cells were seeded in 12-well plates (Corning, USA), each at a concentration of 50000 cells mL⁻¹. The cells were incubated at 5% CO₂, 37 °C and cell proliferation was

monitored. After 24 h, the cells were cultured using fresh culture medium. Aliquots of cell suspension was mixed with an equal volume of 0.4% trypan blue solution and results were counted under a light microscope using a hemocytometer to calculate cell survival rates.

The photo-cytotoxicity of blue, green, and red light irradiation was assessed according to the following method. Cells under the general culture conditions were detached by trypsinization, DMEM/F12 was then added for trypsin deactivation, and cells were centrifuged. The cell pellet was re-suspended in 1 ml DMEM. Cells were stained using a 1:1 ratio of cell suspension to trypan blue, counted using an Invitrogen automated cell counter, and diluted to the appropriate seeding density. For subculture, the seeding density was 5×10^4 cells per well (1 mL volume).

All cells were irradiated for 24 h, and assayed at 48 h. Each condition was applied to one 12-well cell dish. After seeding, the cells were incubated in the dark for 24 h under a humidified 37 °C atmosphere containing 5.0% CO₂. After the 24 h incubation, the cells were irradiated by LED light. The medium was refreshed before the irradiation. The plates were irradiated for 2, 4, or 6 h at 467 nm, or for 6 h at 518 nm and at 630 nm. Following irradiation, cells were cultured for another 24 h under standard conditions. All data analysis was performed from a minimum of three independent experiments.

2.5. Cell apoptosis

Apoptosis of B16F10 melanoma cells was evaluated using a Hoechst 33342 solution under cell fixation. The melanoma cells were fixed with a staining solution (4% paraformaldehyde/PBS) for 10 min. Then, Hoechst was added to the 0.4% diluted Triton X-100 at a ratio of 1: 10000, and the solution was added to the fixed cells in phosphate-buffered saline (PBS) and incubated for 10 min. After PBS rinsing, the cells were incubated with the Hoechst staining solution and observed under a fluorescence microscope. Cells exhibiting bright nuclei or shrinkage under staining represent apoptotic cells. The apoptosis index was defined as the number of apoptotic cells in each image. Five photos were taken of each cell well, and the average number of apoptotic cells was calculated. Cell numbers were determined using ImageJ software.

2.6. Statistical analysis

One-way ANOVA using the Tukey post-hoc test (multiple comparisons) and the two-tailed Student's t-test were performed to evaluate any statistical significance between different groups. Data are presented as the means of the \pm standard deviation (SD), as indicated in the figure captions. All statistical analyses were performed using the Origin 2021 software package. Significance is denoted in the figures as $P < 0.05$ (*), $P < 0.01$ (**), and $P < 0.001$ (***)

3. Results

3.1. Design and fabrication of the optical microneedle patch

The light therapy system introduced in this study is based on an optical microneedle array that provides a transmission access allowing photons to be delivered to the dermis. Subsequently, LED light is irradiated through microneedles inserted into the skin during the designed time to evaluate the effectiveness of the treatment (Fig. 1). Hence, the system used to evaluate the effect of light therapy based on *in vitro* cell experiments in this study has two parts: 1) a microneedle patch fabricated by transparent optical and biodegradable materials that can penetrate the stratum corneum with high mechanical strength, and 2) an LED light irradiation platform of simple design that fits a cell culture dish. The fabricated microneedles should be fixed in the cell culture dish at a certain height to accurately measure the effect of light delivery.

Poly(lactic acid) (PLA) is a versatile biopolymer with biodegradable characteristics that is widely used in the fields of tissue engineering, regenerative medicine, drug carriers, orthopaedic interventions, cancer therapy, and drug delivery [26,27]. Moreover, owing to its low cost, easy

processing, high transparency, and biodegradability, PLA was used in this study as the material for the optical microneedles. The PLA microneedles were fabricated using a hot-embossing method consisting of two steps (Fig. 2(a)). A polydimethylsiloxane (PDMS) negative mold was first fabricated using a commercial steel microneedle patch that provided the necessary height. In this study, microneedles were set as 800 μm in height to avoid any pain that can be caused by microneedles with a height greater than 1 mm, but are capable of penetrating the epidermis to reach the dermis. The fabricated microneedle patch has a thin base approximately 300 μm in thickness, conformable to curved skin surfaces. Each microneedle in the patch is conical in shape with a less than 10 μm tip, a diameter of 200 μm and 800 μm in height (Fig. 2(b)). The PLA material after fabricated by this method was calculated by crystallinity degree as amorphous material (Supplement 1) to provide a high transparent.

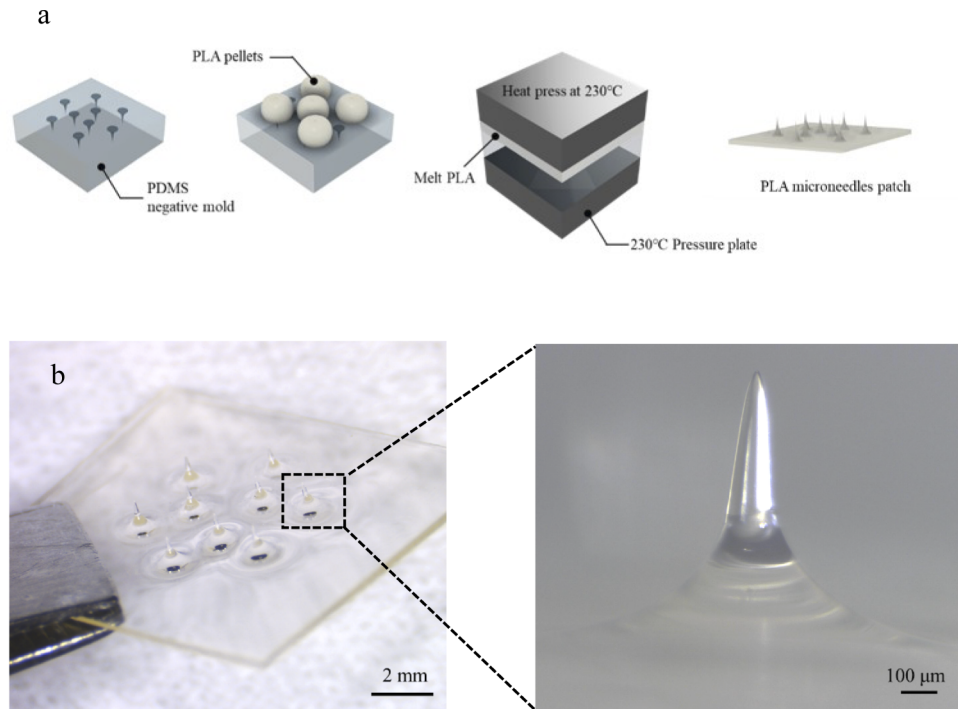


Fig. 2. PLA optical microneedle patch. a, Fabrication process for a PLA microneedle patch. Firstly, prepare the PDMS mold as the negative mold. Add PLA pellets on the PDMS negative mold and heat at 230°C. Then press the melted PLA pellets by 1.5 MPa. Finally, cool them to room temperature then peel the microneedles and attain the microneedle patch. b, Optical image of the fabricated optical PLA microneedle patch with high transparency; the image on the right shows a side view of one microneedle in the fabricated conical microneedle patch with the height of 800 μm , tip diameter of less than 10 μm .

3.2. Properties of PLA microneedle patch

Before evaluating the effect of the microneedle patch with light for *in vitro* assays, the properties of the PLA microneedles were investigated: 1) mechanical strength for penetration of dermal tissue, 2) optical transmission, and 3) biosafety for the *in vitro* experiment. First, we built a force-displacement test station (Fig. 3(a)) and conducted a porcine skin insertion test to verify that the fabricated PLA microneedle patch possessed sufficient mechanical strength to penetrate the skin. A force-displacement sensor was moved downwards on a single microneedle until the

microneedle broke. The force increase versus distance was continually recorded. Result showed that a single PLA microneedle is expected to withstand a buckling force of 1 N before failure, as shown in Fig. 3(a). Although the Young's modulus of human skin varies significantly depending on relative humidity, age, race, body location, etc., the general insertion force needed to puncture the stratum corneum (SC) with a microneedle should be greater than 58 mN [28]. Thus, the microneedle patch we fabricated can puncture human skin successfully.

After penetrating the porcine skin with the microneedle patch, the specimen was stained using Trypan blue (Fig. 3(b)). The results obtained from the side view showed that all microneedles on the patch successfully penetrated the porcine skin and could pierce the SC of the skin to a depth of 500 μm . After the PLA microneedle patch was removed from the porcine skin, the microneedles maintained their conical shape and sharp tips (Supplement 1), further confirming that their mechanical strength was sufficient for subsequent light delivery into the skin.

Optical PLA microneedles can penetrate the skin tissue to provide light access in the skin. As a result, it is important to understand the light transmission in a microneedle and light diffusion in the skin. In a previous report, light was focused at the tip of the microneedle, similar to an optical fiber [16,22,26,29]. As the refractive index of the skin is complex with the opaque property of human skin, it was difficult to observe light emitted from microneedles below the skin. Therefore, we performed a light ray tracing simulation of the microneedle in the skin, with setting the refractive index of PLA and the skin as 1.47 and 1.3, respectively. The microneedle shape in the simulation was set to be the same as the fabricated result. As the reported previously, in the simulation results, the incident light is totally reflected in the microneedle then refracted toward the outside of the microneedle in the tip (Supplement 1). To verify that light can be refracted in the tip, we put a blue LED light behind the microneedle base to test whether the light can be emitted from the tip as the simulation results. As a result, we could clearly observe that the light was concentrated at the tip of the microneedles (Supplement 1). Based on such characteristics of light microneedles, which emit light at the tip of the needle after insertion into the skin, we considered that they can be applied for local introduction of light.

Next, B16F10 murine melanoma cells were cultured in the presence of microneedles for over two days to evaluate the toxicity of the PLA microneedle patch (Fig. 3(c)). Regarding cell viability statistics, no significant difference in cell viability was observed between the control cells and cells added with PLA microneedles (Fig. 3(c)). There was also no significant difference between the control group and the PLA microneedle group in terms of cell morphology (Fig. 3(d)). Both results indicated that the PLA microneedle patch represents a safe approach for *in vitro* testing without affecting cell viability.

3.3. Design and preparation of LED irradiation system for *in vitro* cell tests

To study the effect of light and the microneedle patch during *in vitro* experiments, an LED irradiation system consisting of an LED array, supporting bracket, power supply, and fixed microneedle patch was prepared. To date, several light sources have been used in *in vitro* experiments to verify the effect of light on cell lines [30–35]. However, considering the cost to customize equipment and requirements for the different targets in the experiments, a low cost, easy-to-assemble, simple design, accurate irradiation area, and a power supply that can be installed in an incubator, are desirable. In this study, we designed the LED array for simple and inexpensive fabrication, which requires simple welding and circuit design. A 12-well culture dish was chosen to mimic the area of melanoma lesions. A 3D-printed support bracket was used to adjust the light irradiation distance. In addition, we used a conventional mobile battery to supply electrical power to the entire device (Fig. 4(a)). The whole system was designed to have sufficient air circulation so that the heat produced by the LEDs can escape, avoiding any heating effect on skin cells. To confirm whether other wavelengths of light have the same effect

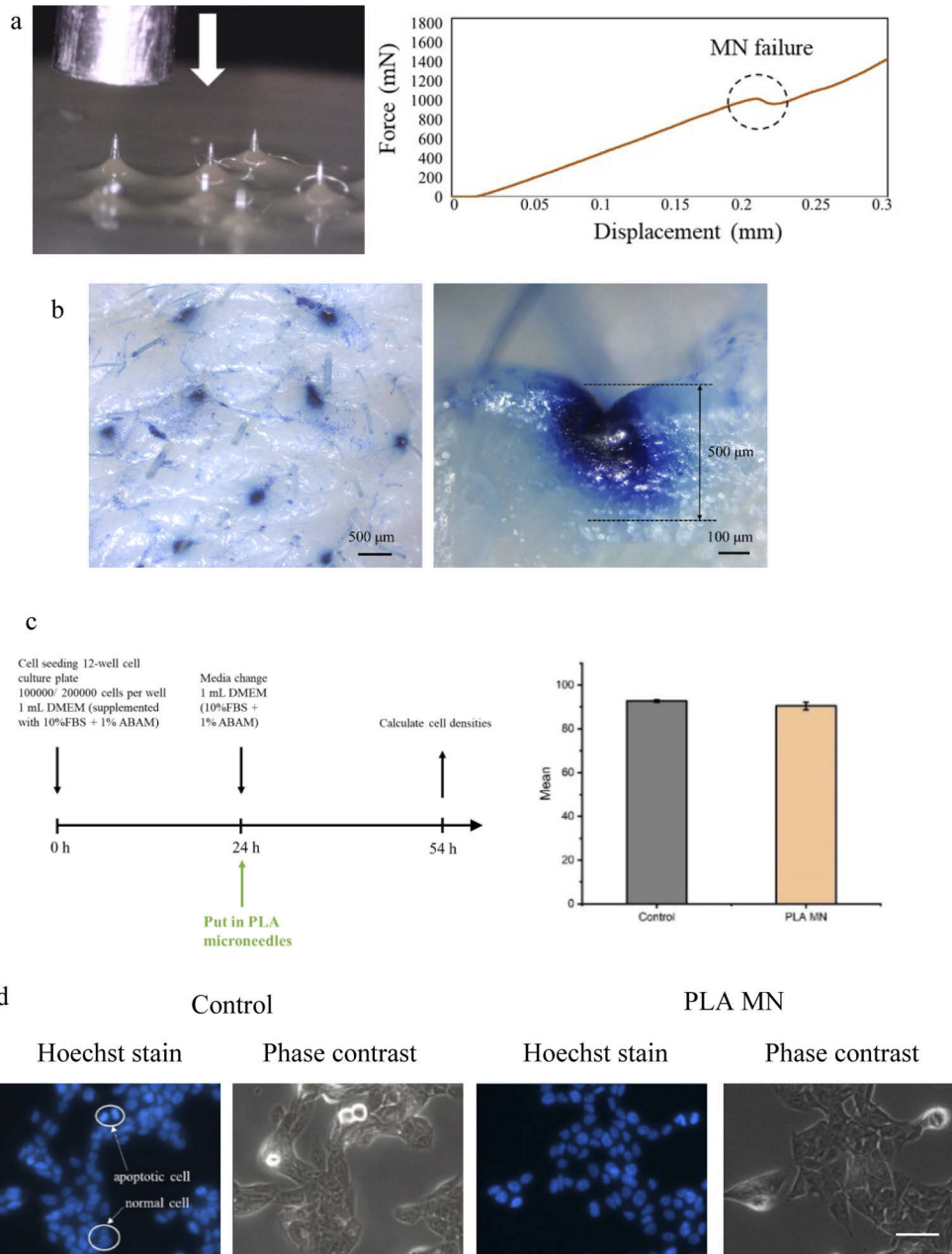


Fig. 3. Properties of PLA microneedle (MN) patch. **a**, Experimental setup for the mechanical behaviour of the microneedle under load and corresponding failure. **b**, Optical image of methylene blue staining of the porcine skin with inserted microneedle patch. Right: side view of skin sample showing the indentation caused by the penetration of a microneedle at a 500 μm depth. **c**, Left: Cell Culture outline and viability of B16F10 cells with PLA microneedle patch over 54 hours. Right: Mean of the \pm standard deviation (SD), $n = 3$ repeated tests. **d**, Fluorescent images of cells stained using Hoechst, control group and cells cultured with PLA microneedles group. Statistical significance was determined by Student's test (Origin 2021). Scale bar: 50 μm .

on B16F10 melanoma cells, three LED arrays using blue, green, and red light were evaluated in the experiments (Fig. 4(d)).

We then designed a microneedle patch that can be fixed in the cell culture to deliver light close to the cells without physically contacting the cells. To prevent the microneedle patch from floating in the culture medium, we introduced a cell culture insert to fix the microneedle patch at the desirable height. Furthermore, areas without microneedles were covered with aluminum foil to accurately evaluate the local effect of the microneedle patch (Fig. 4(b)-(c) and Supplement 1). All devices can be sterilized using alcohol or UV light. Although using our system as a standard experimental method requires further verification, we consider that it provides new concepts as well as idea for future experiments related to cell irradiation using light.

3.4. Apoptosis of B16F10 cells under LED irradiation and irradiance effects without microneedles

To evaluate the effectiveness of blue light on B16F10 cells using our device, we irradiated LED light to B16F10 cells for at least 2 h. The results indicated that cell viability decreased gradually to 82% compared to 91% for the control and that cells exhibited changes in morphology (Fig. 5(b)). It indicated that blue light at 467 nm caused significant light cytotoxicity that induced apoptosis of B16F10 cells. Although the significant difference in viability following irradiation was observed, the percentage of cells that died after two hours of treatment may not be sufficient for clinical applications. Therefore, we next investigated whether increasing the exposure time to blue light can increase the apoptosis of cells. As the irradiation time increased to 4 h and 6 h, the cell viability of B16F10 decreased from 82% at 2 h to 78%, and 72% at 4 and 6 h, respectively, and the number of apoptotic cells were observed using Hoechst staining (Fig. 5(e)). Hoechst staining was used to distinguish apoptotic cells from healthy cells [36].

The mechanism on how blue light can cause apoptosis in melanoma cells is still under investigation. However, one possible theory is that blue light leads to an increase in the mitochondrial membrane potential and in the mitochondria-related apoptotic proteins [30–33]. Owing to the wide variation in experimental setups, the previously published results on light-induced effects on cell viability are difficult to compare. Further evidence is necessary to confirm the mechanisms involved using blue light irradiation, but our results suggest that blue light can induce cell apoptosis.

Because previous studies have demonstrated that LED lights of different wavelengths can also affect skin cells [37,38] we compared the effect of blue light to those of red and green light on B16F10 cells. The cells were irradiated at 467 nm (blue), 518 nm (red), and 630 nm (green) wavelengths, and were compared to the control groups in the dark. Irradiation by blue light resulted in unexpected but substantially reduced cell growth, while green and red light had no noticeable effect, even after 6 h of irradiation (Fig. 5(c)). The results suggested that blue light specifically causes apoptosis in melanoma cells compared to light using other wavelengths.

In the blue light irradiation experiments, we found that some cells were obviously under extreme stress from the change in morphology, although it was difficult to judge whether apoptosis occurred based on the staining results. Therefore, we hypothesised that the cells will gradually become apoptotic after repeated light exposure. On the other hand, considering future clinical practice, 6-hour irradiation may place too great a burden on patients. Therefore, we evaluated whether blue light irradiation can yield better results if irradiated for 2 h per day for a total of 6 h over three consecutive days.

The experimental results showed that the apoptosis rate involving 2 h per day significantly increased in comparison considering the results from the control group as well as the 6-hour continuous irradiation groups, (Fig. 5(d)). At the same time, comparing the total number of cells, irradiation for 2 h a day obviously inhibited the growth rate of malignant cells, which was especially significant when compared to the control group (Supplement 1).

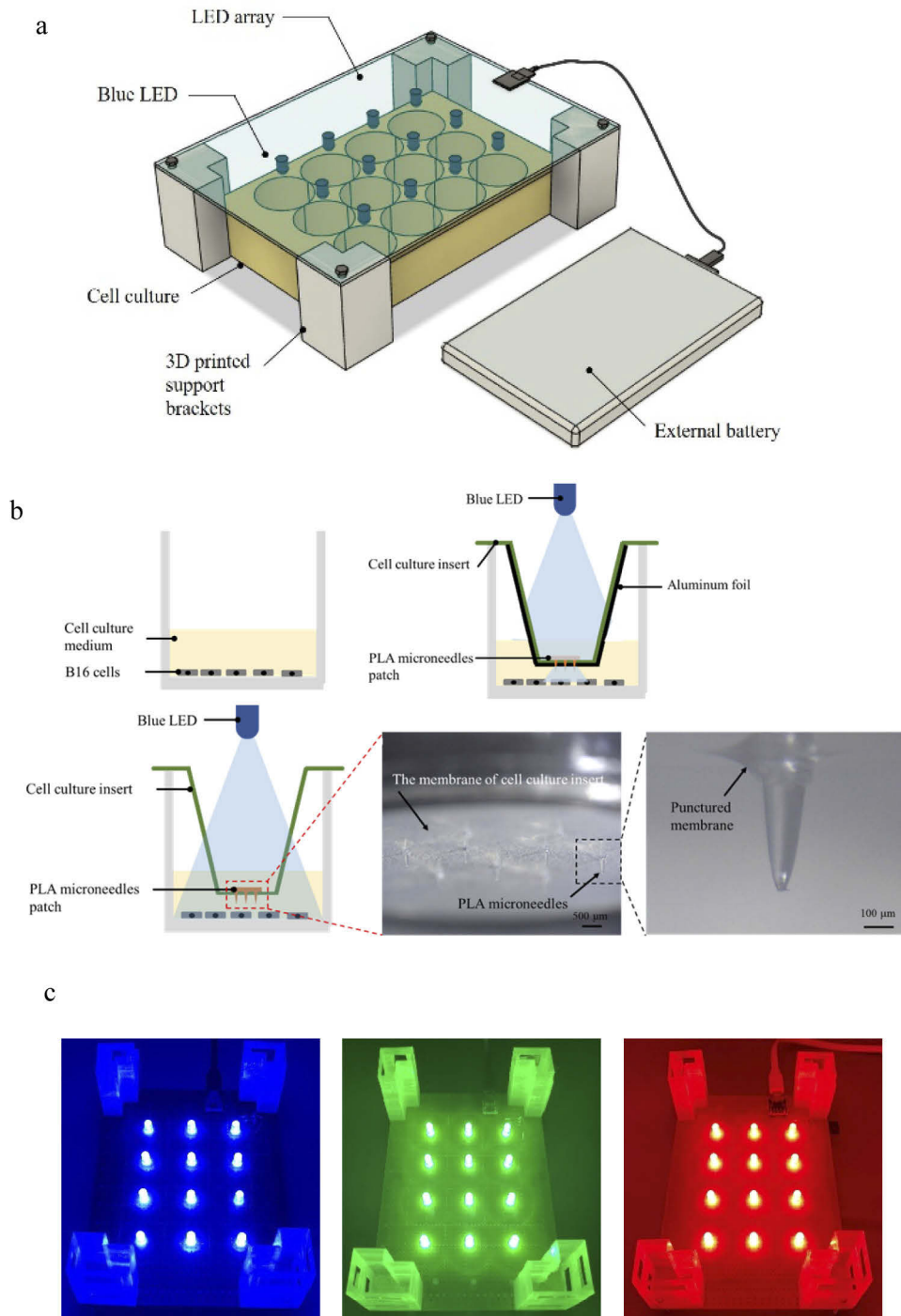


Fig. 4. LED setup of the *in vitro* cell irradiation system. a, Schematic of LED array on a printed circuit board (PCB) equipped with 3D printed support brackets to ensure adequate distance between the LED array and cell culture. A mobile power supply can also be placed in the incubator. b, Schematic diagram of PLA microneedles fixed on a cell culture insert. Microneedles puncture the membrane of the cell culture insert. c, Blue, green, and red 12-LED arrays mounted on PCBs.

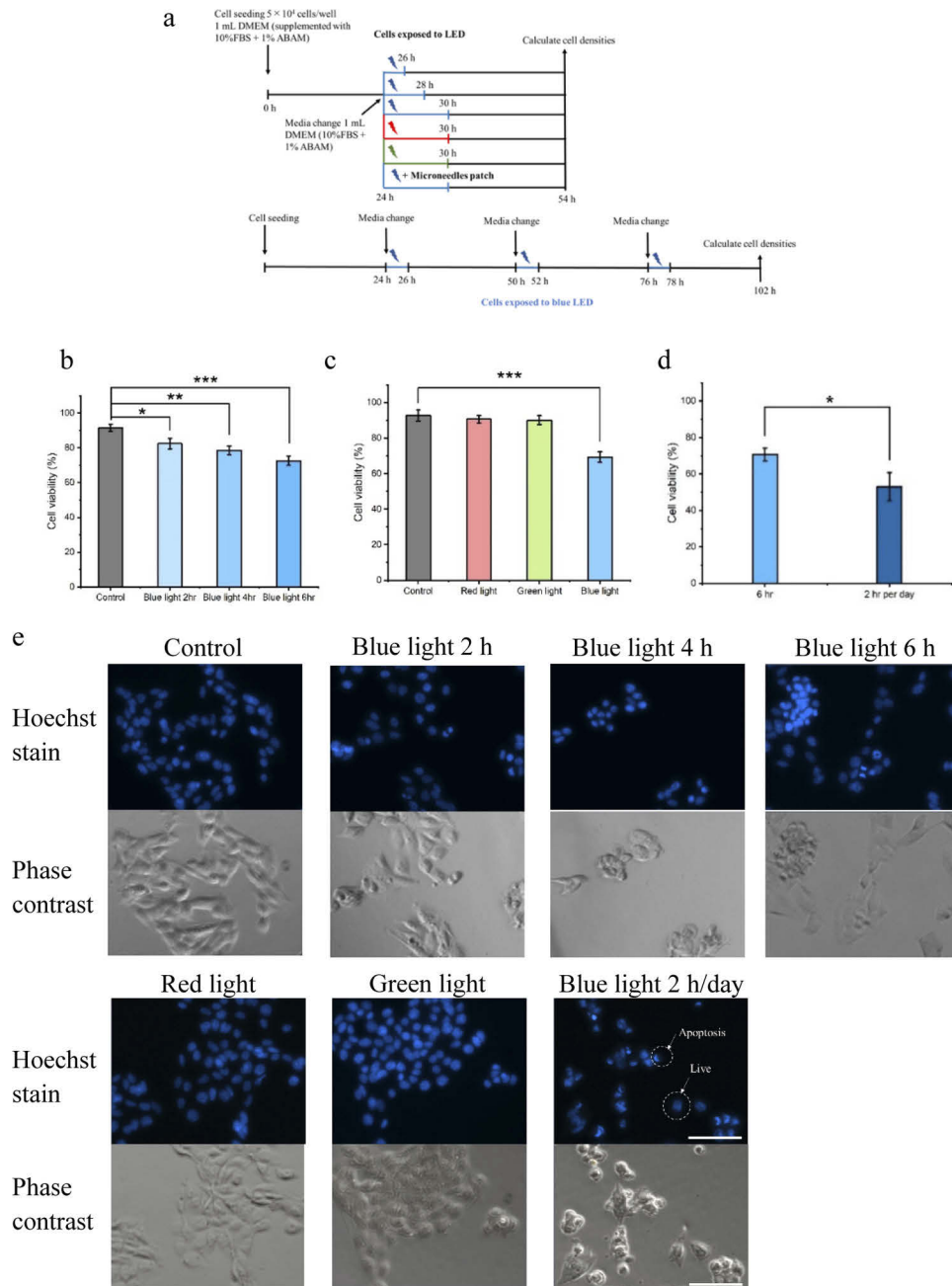


Fig. 5. Effect of B16F10 cell exposure to different wavelength LEDs. **a**, Culture outline of B16F10 cells under exposure to LED light. **b**, Cell viability of B16F10 cells after exposure to blue LED light for 2 h, 4 h, and 6 h. **c**, Cell viability of B16F10 cells irradiated by red light and green light for 6 h, respectively. **d**, Cell viability of B16F10 cells under repeated exposure for 2 h per day using blue LED light (3 consecutive days). **e**, Fluorescent images of cells stained by Hoechst solution for control group and cells exposed to LED light. Data represent the mean values of the \pm SD of three ($n=3$) independent experiments. Statistical significance was determined based on, $p < 0.05$ (*), $p < 0.01$ (**), and $p < 0.001$ (***) by one-way ANOVA with Tukey's post hoc test for multiple comparisons and Student's test (Origin 2021). Scale bar: 50 μ m.

No statistically significant effect was observed when the cells were for irradiated for 2 h at once (Supplement 1). However, repeated irradiation over a short time (2 h, 3 times) induced more apoptosis than 6 h once, which means a better therapeutic effect. In other words, for a better treatment effect, the best treatment time (light dose) should be explored further with respect to clinical settings, as long treatment times appear to produce stagnant effects and cause unnecessary discomfort for patients.

3.5. Effect of optical microneedles using blue LED light

As mentioned earlier, the effect of blue light irradiation on melanoma cells was verified. However, for clinical trials in the future, the limited penetration depth due to the optical characteristics of skin represents a difficult obstacle to overcome. The conventional treatment option is to increase the light power with the expectation that high energy will deliver more photons into the skin, but it can lead to side effects such as skin burns and pain. However, it is considered that the optical microneedle technique can both minimize the damage associated with invasive procedures and deliver light at the target depth. For melanoma skin cancer, the target depth can be up to 2 mm deep in the skin. But it is obvious that during treatment, effective blue light cannot reach the

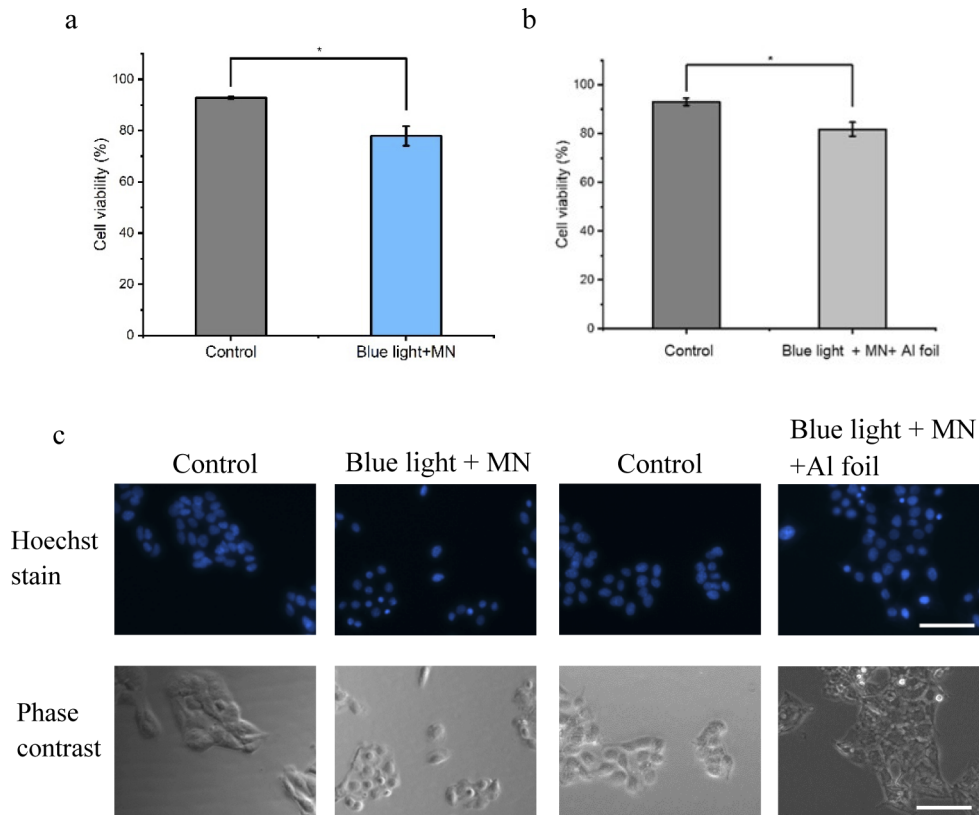


Fig. 6. Effects of optical microneedles and a blue LED light. a, Viability of B16F10 cells after exposure to blue LED light using microneedle patch. b, Viability of B16F10 cells after exposure to blue LED light and microneedle patch and aluminum foil. c, Fluorescent images of cells stained by Hoechst solution for control group and microneedles group with microneedle patch. Data represent the mean values of \pm SD of three ($n=3$) independent experiments. Statistical significance was determined at $p < 0.05$ (*), $p < 0.01$ (**), and $p < 0.001$ (***) by the Student's test (Origin 2021). Scale bar: 50 μ m.

target depth and the light transmission efficiency is relatively low, because the light was absorbed, reflected and refracted by the skin tissue. Therefore, optical microneedles was considered as a device to deliver light in to target depth with low invasive.

To determine the effect of the light and microneedle patch, we used PLA microneedles fixed on an insert without light as the control group to evaluate blue light delivery using a microneedle patch, as well as a PLA microneedle patch fixed on the insert and then blocked with aluminum foil as a second control group. The former confirmed that blue light can penetrate PLA materials well and has an effect on cell activity. The latter used aluminum foil to block out all light except for microneedles in order to accurately measure the local therapeutic effect of the optical microneedle (whether the light from the low-intensity LED has difficulty penetrating the skin). In other words, the second control was used to determine whether the light emitted from the tip of the microneedle based on the characteristics of real skin has an inhibitory effect on B16F10 cells.

After irradiation for 6 h, the cell viability of B16F10 cells was significantly lower than that of the control group, indicating that blue light was successfully transmitted from the PLA microneedles to cells below the membrane of inserts. It was verified that blue light can induce the apoptosis of melanoma cells, but the side effect on healthy skin cells should be also verified. The max light dose of our experiments was 146.9 J/cm^2 , less than the report of light dose blue light toxic on skin cells (human keratinocytes and skin-derived endothelial cells) 500 J/cm^2 [39]. However, we noted that for the same irradiation time using blue light, the PLA microneedles with the insert yielded higher cell viability. Such result was considered to be possible because the insert is not totally transparent, similar to the PLA microneedle patch (as a high transparent optical material, PLA has 94% transparency [40,41]). However, even though the film of the insert reduces the light energy, the effect of blue light still produces a significant difference after irradiation for 6 h. The same experiment was performed on the microneedles blocked by aluminum foil. Although the aluminum foil covered all light except for the light irradiated from the PLA microneedles, there was still a significant difference in cell viability compared to the control group. The results indicate that the microneedles can deliver light to the cells directly, and the light from the microneedle tips has a certain therapeutic effect because it induces cell apoptosis (Fig. 6(a)-(b)).

In addition, we stained the cells to observe cells in the localised area influenced by optical microneedles to verify the localised light irradiation of microneedles. Overall, the results indicated that the microneedle patch can deliver light successfully and can be used for localised treatment using blue light on B16F10 cells (Fig. 6(a)-(c)).

4. Discussion

In the treatment for melanoma, drug resistance to conventional therapies has always been considered as a bottleneck. In addition, oral treatments are associated with undesirable side effects and low efficiency, whereas traditional laser treatments are associated with local epidermal burns. Phototherapy and photodynamic therapy are emerging melanoma treatments with minimal systematic side effects and also reduce the expected epidermal burns. Therefore, there has been continuous demand for new, effective apoptosis-inducing treatments with fewer side effects. In the present study, we proposed microneedle with blue LED as the new treatment method. It is a light system using optical microneedles as a localised treatment light waveguide device and the blue LED was confirmed to have effects on melanoma B16F10 cells. In addition, we developed an LED irradiation system for photobiological *in vitro* tests including low cost, easy design, and reliability. Herein, optical microneedles for an *in vitro* light delivery test designed with a cell culture insert was also a novel testing method. To verify that optical microneedle is an effective treatment, we used our irradiation system and protocol to test the effect of visible light on cancer cell lines and showed an example of *in vitro* Hoechst dye testing and PI staining (Supplement 1).

After evaluating various irradiation times (dose) and wavelengths on B16F10 murine melanoma cells, blue light was verified to induce certain toxicity in the melanoma cells, indicating its potential for clinical melanoma treatment. When microneedles were inserted into the cell culture as a localization light delivery device, it still is able to induce the apoptosis of B16F10 melanoma cells, which suggests that localised therapy is possible. Since the microneedles directly guide light into the cells, the extremely low-energy LED used in this experiment still has the effect of inducing apoptosis. Therefore, it is foreseeable to reduce side effects such as burns caused by excessive light energy in the future.

Only a few studies have explored the effect of blue light on skin cancer. Previous studies changed the dose and wavelength to demonstrate the effectiveness of blue light and the relationship between blue light and ROS produced by mitochondria [27–32]. There are also some reports for UV light and different wavelengths of blue light from 418 nm to 476 nm to explore the optimal wavelength for light therapy on skin cancer [37]. The research has better helped us understand the theory for the effects of blue light on melanoma. However, in addition to the principle studies, deeper light-guiding and less damaging therapeutic aids for local treatment will further advance the possibility of clinical application of blue light. The painless and less invasive advantages of the micron structure of the microneedle itself, as well as the ability to direct light deeper into the skin after piercing the epidermis, represent a good prospect for optical microneedle in the field of light therapy. In particular, this study fills the data support for the *in vitro* experimental part of the optical microneedle, from the effect of blue light to the light results after adding microneedles, and the effect of PLA microneedle material on the experimental results. The cell growth inhibition resulting from repeated exposure to light, together with the local irradiation of optical microneedles, is an alternative treatment for patients who suffer from prolonged treatment with extensive side effects.

In the future, the applications of microneedles for light delivery should be further tested, including optimization of the height, needle array, and diameter of microneedles. In addition, for the application of optical microneedle as a light waveguide, a detailed characterization of losses, propagation mode polarization studies should be performed extensively and discussed [41,42]. Simulation and free space experiments with a fiber-coupled laser and a high-resolution camera are necessary before *in vivo* experiments. For future industrial production, faster, large-area, and low-cost production methods also need to be discussed. In addition to the hot embossing technique used in this study as a widely used industrial production method, methods such as electro-drawn lithography can also be applied in the field of optical microneedles [20].

Furthermore, the evaluation and characterization of the mechanisms that produces the blue light effect using microneedles on melanoma cells will be important for further clinical applications. Moreover, thermos-optical analyses should also be assessed as a result of long time irradiation. Heat may be absorbed by the skin and the microneedle may result to side effects such as burns. It is thus essential to find a light source that is powerful enough and yet does not cause heat damage with various irradiations and types of LED for future application. Blue light induced apoptosis of melanoma tumor cells, but also inhibited cell differentiation and growth, and the analysis of growth rates over 72 hours also needed further validation [31]. At the same time, we consider that more evidences, not only *in vitro* but also *in vivo*, should be gathered and evaluated. Optical microneedles remain a novel idea that has not received great attention, but we believe that the technology demonstrated here has potential significance for propelling the technology towards clinical applications. The results shown in our study will provide a new direction to choose proper treatment methods of phototherapy for skin cancer as well as other skin diseases such as acne, psoriasis, and perhaps internal cancers as well.

The results shown in our study will provide a new direction to choose proper treatment methods of phototherapy for skin cancer as well as other skin diseases such as acne, psoriasis, and perhaps internal cancers as well.

Funding. JSPS Core-to-Core program A (grant No. JPJSCCA20190006).

Acknowledgments. This research was supported by the JSPS Core-to-Core program A (grant No. JPJSCCA20190006). We thank Prof. Kazuaki Kudo (Institute of Industrial Science, The University of Tokyo) for his assistance with research supports for experiment materials as well as human resources. The authors appreciate Heyi Jing and Qin Boyu (The University of Tokyo) for their advice during experiments.

Disclosures. The authors declare no competing interests.

Data availability. All data are available in the main text or the supplementary materials.

Supplemental document. See [Supplement 1](#) for supporting content.

References

1. D. Schadendorf, D. E. Fisher, C. Garbe, J. E. Gershenwald, J.-J. Grob, A. Halpern, M. Herlyn, M. A. Marchetti, G. McArthur, A. Ribas, A. Roesch, and A. Hauschild, "Melanoma," *Nat. Rev. Dis. Primers.* **1**(1), 15003 (2015).
2. G. C. Leonardi, L. Falzone, R. Salemi, A. Zanghi, D. A. Spandidos, J. A. Mccubrey, S. Candido, and M. Libra, "Cutaneous melanoma: from pathogenesis to therapy (Review)," *Int. J. Oncol.* **52**(4), 1071–1080 (2018).
3. C. Lee, F. Collichio, D. Ollila, and S. Moschos, "Historical review of melanoma treatment and outcomes," *Clin. Dermatol.* **31**(2), 141–147 (2013).
4. B. Domingues, J. M. Lopes, P. Soares, and H. Pópulo, "Melanoma treatment in review," *Immunotargets Ther.* **7**, 35–49 (2018).
5. L. E. Davis, S. C. Shalin, and A. J. Tackett, "Current state of melanoma diagnosis and treatment," *Cancer Biol. Ther.* **20**(11), 1366–1379 (2019).
6. M. Lalan, P. Shah, K. Barve, K. Parekh, T. Mehta, and P. Patel, "Skin cancer therapeutics: nano-drug delivery vectors-present and historical beyond," *Future J. Pharm. Sci.* **7**(1), 179 (2021).
7. M. Aris and M. M. Barrio, "Combining immunotherapy with oncogene-targeted therapy: a new road for melanoma treatment," *Front. Immunol.* **6**, 46 (2015).
8. M. R. Hamblin, "Mechanisms and applications of the anti-inflammatory effects of photobiomodulation," *AIMS Biophys.* **4**(3), 337–361 (2017).
9. C. Naidoo, C. A. Kruger, and H. Abrahamse, "Photodynamic therapy for metastatic melanoma treatment: a review," *Technol. Cancer Res. Treat.* **17**, 153303381879179 (2018).
10. G. Ablon, "Phototherapy with light emitting diodes," *J. Clin. Aesthet. Dermatol.* **11**(2), 21–27 (2018).
11. P. Zhang and M. X. Wu, "A clinical review of phototherapy for psoriasis," *Lasers Med Sci.* **33**(1), 173–180 (2018).
12. Z. Chen, S. Huang, and M. Liu, "The review of the light parameters and mechanisms of photobiomodulation on melanoma cells," *Photodermatol. Photoimmunol. Photomed.* **38**(1), 3–11 (2022).
13. P.-S. Oh, K. S. Na, H. Hwang, H.-S. Jeong, S. Lim, M.-H. Sohn, and H. J.- Jeong, "Effect of blue light emitting diodes on melanoma cells: Involvement of apoptotic signaling," *J Photochem Photobiol B.* **142**, 197–203 (2015).
14. T. Lister, P. A. Wright, and P. H. Chappell, "Optical properties of human skin," *J Biomed Opt.* **17**(9), 0909011 (2012).
15. A. N. Bashkatov, E. A. Genina, V. I. Kochubey, and V. V. Tuchin, "Optical properties of human skin, subcutaneous and mucous tissues in the wavelength range from 400 to 2000nm," *J. Phys. D: Appl. Phys.* **38**(15), 2543–2555 (2005).
16. S. L. Hopkins, B. Siewert, S. H. C. Askes, P. Veldhuizen, R. Zwier, M. Heger, and S. Bonnet, "An in vitro cell irradiation protocol for testing photopharmaceuticals and the effect of blue, green, and red light on human cancer cell lines," *Photochem. Photobiol. Sci.* **15**(5), 644–653 (2016).
17. M. Kim, J. An, K. S. Kim, M. Choi, M. Humar, S. J. J. Kwok, T. Dai, and S. H. Yun, "Optical lens-microneedle array for percutaneous light delivery," *Biomed. Opt. Express* **7**(10), 4220–4227 (2016).
18. P. Makvandi, R. Jamaledin, G. Chen, Z. Baghbantargarhdari, E. N. Zare, C. D. Natale, V. Onesto, R. Vecchione, J. Lee, F. R. Tay, P. Netti, V. Mattoli, A. Jaklenec, Z. Gu, and R. Langer, "Stimuli-responsive transdermal microneedle patches," *Mater. Today.* **47**, 206–222 (2021).
19. L. Wu, P. Shrestha, M. Iapichino, Y. Cai, B. Kim, and B. Stoeber, "Characterization method for calculating diffusion coefficient of drug from microneedles into the skin," *J Drug Deliv Sci Technol.* **61**, 102192 (2021).
20. S. Coppola, V. Vespini, G. Nastì, and P. Ferraro, "Transmitting light through biocompatible and biodegradable drug delivery micro needles," *IEEE J. Select. Topics Quantum Electron.* **27**(5), 1–8 (2021).
21. F. Ruggiero, R. Vecchione, S. Bhowmick, G. Coppola, S. Coppola, E. Esposito, V. Lettera, P. Ferraro, and P. A. Netti, "Electro-drawn polymer microneedle arrays with controlled shape and dimension," *Sensors and Actuators B: Chemical* **255**(2), 1553–1560 (2018).
22. R. Vecchione, S. Coppola, E. Esposito, C. Casale, V. Vespini, S. Grilli, P. Ferraro, and P. A. Netti, "Electro-drawn drug-loaded biodegradable polymer microneedles as a viable route to hypodermic injection," *Adv. Funct. Mater.* **24**(23), 3515–3523 (2014).
23. M. Battisti, R. Vecchione, C. Casale, F. A. Pennacchio, V. Lettera, R. Jamaledin, M. Profeta, C. D. Natale, G. Imparato, F. Urciuolo, and P. A. Netti, "Non-invasive production of multi-compartmental biodegradable polymer microneedles for controlled intradermal drug release of labile molecules," *Front. Bioeng. Biotechnol.* **7**, 296 (2019).
24. H. Zhang, H. Zhao, X. Zhao, C. Xu, D. Franklin, A. Vázquez-Guardado, W. Bai, J. Zhao, K. Li, G. Monti, W. Lu, A. Kobeissi, L. Tian, X. Ning, X. Yu, S. Mehta, D. Chanda, Y. Huang, S. Xu, B. E. P. White, and J. A. Rogers,

- “Biocompatible light guide-assisted wearable devices for enhanced UV light delivery in deep skin,” *Adv. Funct. Mater.* **31**(23), 2100576 (2021).
25. Y. Lee, T. Kang, H. R. Cho, G. J. Lee, O. K. Park, S. Kim, B. Lee, H. M. Kim, G. D. Cha, Y. Shin, W. Lee, M. Kim, H. Kim, Y. M. Song, S. H. Choi, T. Hyeon, and D.-H. Kim, “Localized delivery of theranostic nanoparticles and high-energy photons using microneedles-on-bioelectronics,” *Adv. Mater.* **33**(24), 2100425 (2021).
 26. Y. Ramot, M. Haim-Zada, A. J. Domb, and A. Nyska, “Biocompatibility and safety of PLA and its copolymers,” *Adv. Drug Deliv. Rev.* **107**, 153–162 (2016).
 27. L. Wu, J. Park, Y. Kamaki, and B. Kim, “Optimization of the fused deposition modeling-based fabrication process for polylactic acid microneedles,” *Microsyst. Nanoeng.* **7**(1), 58 (2021).
 28. J.-H. Park, M. G. Allen, and M. R. Prausnitz, “Biodegradable polymer microneedles: fabrication, mechanics and transdermal drug delivery,” *J. Controlled Release.* **104**(1), 51–66 (2005).
 29. M. Kang, C. Shim, S. Na, B. Lee, N. L. Jeon, and H. Yun, “Improved cosmeceutical phototherapy using microneedle,” *Microsyst. Technol.* **25**(7), 2547–2552 (2019).
 30. T. Niu, Y. Tian, Z. Mei, and G. Guo, “Inhibition of autophagy enhances curcumin united light irradiation-induced oxidative stress and tumor growth suppression in human melanoma cells,” *Sci. Rep.* **6**(1), 31383 (2016).
 31. M. Ohara, Y. Kawashima, O. Katoh, and H. Watanabe, “Blue light inhibits the growth of B16 melanoma cells,” *Jpn. J. Clin. Oncol.* **93**(5), 551–558 (2002).
 32. K. Sato, Y. Minai, and H. Watanabe, “Effect of monochromatic visible light on intracellular superoxide anion production and mitochondrial membrane potential of B16F10 and B16F10 murine melanoma cells,” *Cell Biol. Int.* **37**(6), 633–637 (2013).
 33. R. A. Akasov, N. V. Sholina, D. A. Khochenkov, A. V. Alova, P. V. Gorelkin, A. S. Erofeev, A. N. Generalova, and E. V. Khaydukov, “Photodynamic therapy of melanoma by blue-light photoactivation of flavin mononucleotide,” *Sci. Rep.* **9**(1), 9679 (2019).
 34. Z. Chen, W. Li, X. Hu, and M. Liu, “Irradiance plays a significant role in photobiomodulation of B16F10 melanoma cells by increasing reactive oxygen species and inhibiting mitochondrial function,” *Biomed. Opt. Express* **11**(1), 27–39 (2020).
 35. C. Chamayou-Robert, C. DiGiorgio, O. Brack, and O. Doucet, “Blue light induces DNA damage in normal human skin keratinocytes,” *Photodermatol Photoimmunol Photomed.* **38**(1), 69–75 (2022).
 36. L. C. Crowley, B. J. Marfell, and N. J. Waterhouse, “Analyzing cell death by nuclear staining with Hoechst 33342,” *Cold Spring Harb Protoc.* **2016**, 9 (2016).
 37. A. Cios, M. Ciepielak, Ł. Szymański, A. Lewicka, S. Cierniak, W. Stankiewicz, M. Mendrycka, and S. Lewicki, “Effect of different wavelengths of laser irradiation on the skin cells,” *Int. J. Mol. Sci.* **22**(5), 2437 (2021).
 38. A. Sparsa, K. Faucher, V. Sol, H. Durox, S. Boulinguez, V. Doffoel-Hantz, C.-A. Calliste, J. Cook-Moreau, P. Krausz, F. G. Sturtz, C. Bedane, M.-O. Jauberteau-Marchan, M.-H. Ratinaud, and J.-M. Bonnetblanc, “Blue light is phototoxic for B16F10 murine melanoma and bovine endothelial cell lines by direct cytotoxic effect,” *Anticancer Res.* **30**(1), 143–147 (2010).
 39. J. Liebmann, M. Born, and V. Kolb-Bachofen, “Blue-light irradiation regulates proliferation and differentiation in human skin cells,” *Journal of Investigative Dermatology.* **130**(1), 259–269 (2010).
 40. R. Auras, B. Harte, and S. Selke, “An overview of polylactides as packaging materials,” *Macromol Biosci.* **4**(9), 835–864 (2004).
 41. S. Nizamoglu, M. C. Gather, M. Humar, M. Choi, S. Kim, K. S. Kim, S. K. Hahn, G. Scarcelli, M. Randolph, R. W. Redmond, and S. H. Yun, “Bioabsorbable polymer optical waveguides for deep-tissue photomedicine,” *Nat Commun* **7**(1), 10374 (2016).
 42. C. Wu, X. Liu, and Y. Ying, “Soft and stretchable optical waveguide: light delivery and manipulation at complex biointerfaces creating unique windows for on-body sensing,” *ACS Sens.* **6**(4), 1446–1460 (2021).